Proceedings of the 4th International Congress APMAS2014, April 24-27, 2014, Fethiye, Turkey

Hydroxyapatite Lanthanum Oxide Composites

Y. Bozkurt[a], S. Pazarlioglu[b,*], H. Gokce[c], I. Gurler[d], S. Salman[e]

[a]Marmara University, Technology Faculty, Metallurgy and Materials Engineering Department, 34722 Istanbul, Turkey

[b]Marmara University, Technical Education Faculty, Metal Education Deparment, Goztepe Campus, 34722, Istanbul/ Turkey

[c]Istanbul Technical University, Prof. Dr. Adnan Tekin Material Science & Production Technologies Applied Research Center, 34469 Istanbul/ Turkey

[d]Marmara University, Institute of Pure and Applied Sciences, Metal Education Deparment, 34722 Istanbul/ Turkey

[e]Mehmet Akif Ersoy University, Faculty of Engineering & Architecture, Mechanical Engineering Department, Istiklal Campus, 15100, Burdur/Turkey

In the present study a commercially synthetic hydroxyapatite powders (CSHAp) were doped with lanthanum oxide (5 and 10 wt.% La_2O_3). The composite powders were well homogenized and pelleted in an uniaxial mould at 350 MPa. Pelleted green bodies were sintered at five different temperatures. Finally, the effect of La_2O_3 amount on the microstructural and mechanical properties of CSHA was investigated. Microstructural properties were detected by X-ray diffraction patterns (XRD) and scanning electron microscope (SEM). Mechanical properties of the sintered samples were determined by the density, hardness and compression strength measurements. Experimental results show that the mechanical properties of HA can be improved by the doping of La_2O_3

DOI: 10.12693/APhysPolA.127.1407

PACS: 87.85.jf

1. Introduction

The number of treated skeletal deficiencies steadily increases in a global scale due to accident/injury and/or bone defects. Although autogenous bone is most preferred for the treatment of bone defects, there are disadvantages and risks involved in using autogeneic bone such as post-operation pain, increased blood loss, secondary surgical wounds and risk of thrombosis. Allograft bone could overcome the above limitations, but it bears the risk of transmission of infection (e.g. HIV, Hepatitis, etc.). Another possible alternative is the use of effective and inexpensive biomaterials such as HA produces from different sources such as biologically derived and synthetic hydroxyapatite [1–3]. Despite of its desirable properties, the low fracture strength and poor fatigue resistance due to the instability of OH groups limit the use of its biomedical applications to non-load bearing applications. Low mechanical properties of HA can be improved by precise control of the microstructure and the use of various reinforcements [4–6]. One of the most commonly used methods to improve the mechanical properties of HA, reinforcements of its with oxide based ceramics such as ZrO_2 [7], TiO_2 [8], Al_2O_3 [9], MgO [10], $BaTiO_3$ [11] etc. In the present study, we doped a commercially synthetic hydroxyapatite powder with lanthanum oxide and the effect of lanthanum oxide on the microstructural and mechanical properties of CSHA was investigated.

2. Materials and method

2.1. Materials

A commercial HA powder (5 μm, CAS Number: 1306-06-5, Across Organics/Belqium) was used as matrix material and doped with lanthanum oxide (5 μm, La_2O_3, 5 and 10 wt.%, CAS Number: 1312-81-8, Sigma Aldrich, Germany). The powders were firstly well homogenized in Restch PM 100 ball milling device in a zirconia coated stainless steel container with 15 zirconia balls and enough ethyl alcohol at 180 rpm for 2 h. Afterwards, they were pelleted at 350 MPa according to a British Standard for compression tests [12]. Finally, the compacted green samples were sintered at 900, 1000, 1100, 1200 and 1300 °C for 4 h with the heating and the cooling rates of 5 °C/min.

2.2. Mechanical properties

Density of the sintered samples was calculated using Archimedes method. Relative densities of the sintered samples were calculated by comparing the measured densities with the theoretical densities of samples. (HA: 3.156 g/cm^3, HA-2.5La_2O_3: 3.197 g/cm^3, HA-5La_2O_3: 3.239 g/cm^3 and HA-10La_2O_3: 3.327 g/cm^3) The compression strengths of the samples were measured using Devotrans Universal testing device at 2 mm/min speeds. Micro-vickers indentation method was used to determine the hardness of the sintered samples under the loads of 1.962 N for 20 s.

*corresponding author; e-mail: spazarlioglu@marmara.edu.tr

2.3. Microstructural properties

XRD patterns were obtained at room temperature in an X'Pert MPD Philips diffractometer using Cu-Kα radiation in the range of 2θ (10–90°). The microstructures of the samples were determined by scanning electron microscope (SEM, JOEL Ltd., JSM-5910 LV) after gold coating.

3. Results and discussion

The XRD patterns of CSHA and CSHA-La_2O_3 composites are shown in Fig. 1. All peaks are compatible with HA (JCPDS file no.: 98-006-0428) and no other phases were detected for CSHA samples sintered between 900 °C and 1100 °C. But, the samples sintered at higher temperatures betatricalcium phosphate (β-TCP, at 1200 °C) and beta/alphaTCP and also calcium oxide (β-TCP, α-TCP and CaO, at 1300 °C) phases were determined in addition to HA as shown in Fig. 1a. For all CSHA-La_2O_3 composites were detected HA, lanthanum hydroxide ($La(OH)_3$) and La_2O_3 phases sintered at 900 °C. However, new phases were also detected as summarized in Table and also shown in Fig. 1b, 1c and 1d in addition to the specified phases. Same phases were also detected by F. Oktar *et al.* [13].

TABLE Phases occured during sintering process into CSHA-La_2O_3 composites.

T [°C]	CSHA-2.5La_2O_3	CSHA-5La_2O_3	CSHA-10La_2O_3
900	HA, $La(OH)_3$ and La_2O_3		
1100	HA, La_2O_3 ($H_8La_1O_7P_3$)	HA, La_2O_3, $H_2Ca_3O_9P_2$ and $(Ca(OH)_2$	HA, $La(OH)_3$ $Ca_9(PO_4)_6(PO_3OH)$
1300	HA, La_2O_3, $Ca(OH)_2$	HA, La_2O_3, $(Ca(OH)_2$ and CaO	CaO, La_2O_3 and $Ca_9(PO_4)_6(PO_3OH)$

As shown in Fig. 2 that necks started to form and grow between particles at 900 °C (Fig. 2a1, 2a2 and 2a3), tubular pores appeared along the grain boundaries at 1100 °C (Fig. 2b1, 2b2 and 2b3) and the tubular pores break up into isolated quasi-spherical pores typically located at the triple points of grains at 1300 °C (Fig. 2c1, 2c2 and 2c3). However, grain size decrease by increasing La_2O_3 rates so porous microstructures occured for CSHA-10La_2O_3 composites compared to other La_2O_3 reinforced samples.

As shown in Fig. 3, the density of all sintered samples increase by ascending sintering temperatures. While the lowest density value was obtained for CSHA-10La_2O_3 samples (1.82 ± 0.04 g/cm^3) sintered at 900 °C, the highest density value was obtained for CSHA-2.5La_2O_3 samples (3.06 ± 0.03 g/cm^3) sintered at 1300 °C. It is also seen that density values of CSHA-2.5La_2O_3 composites are higher than other CSHA-La_2O_3 composites. For all sintering temperatures density of CSHA-La_2O_3 composites decrease by increasing La_2O_3 rates which may related to at higher La_2O_3 values diffusion rates. This situation causes the formation of higher porosity. This may be related to particle size of starting powders, milling time, speed and also ball diameters and numbers used during ball milling process.

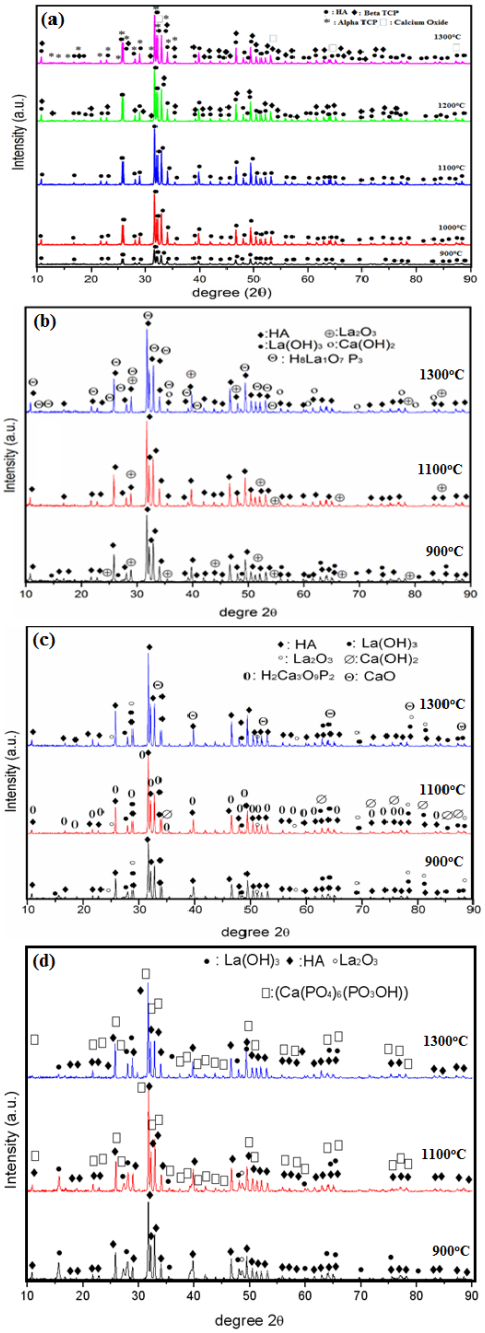

Fig. 1. XRD patterns of (a) pure CSHA, (b) CSHA–2.5La_2O_3 (c) CSHA-5La_2O_3 and CSHA-10La_2O_3 composites.

As shown in Fig. 4, the compressive strength of all samples increase by increasing sintering temperatures until 1100 °C and then decrease at higher sintering temperatures. While the highest compressive strength was obtained to CSHA-5La_2O_3 composites sintered (151 ± 5.56 MPa), the lowest density value was obtained to pure CSHA sintered at 1300 °C (65 ± 5.59 MPa). Compressive strength of pure CSHA decrease at 1200 and 1300 °C because of the formation of TCP, whitlockite and CaO phases, respectively. These formations were also detected to CSHA-La_2O_3 composites, but they have

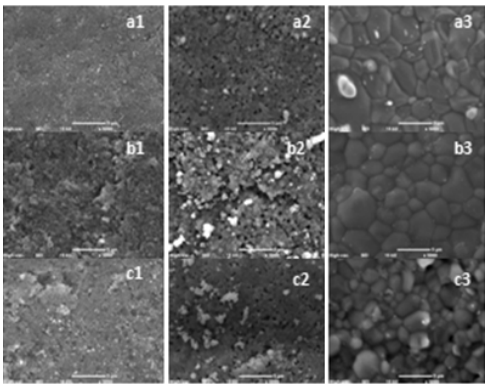

Fig. 2. SEM migrographs of CSHA-2,5La_2O_3 composites sintered at 900 °C (a1), sintered at 1100 °C (a2), sintered at 1300 °C (a3), CSHA-5La_2O_3 composites sintered at 900 °C (b1), sintered at 1100 °C (b2), sintered at 1300 °C (b3) and CSHA-10La_2O_3 composites sintered at 900 °C (c1), sintered at 1100 °C (c2), sintered at 1300 °C (c3).

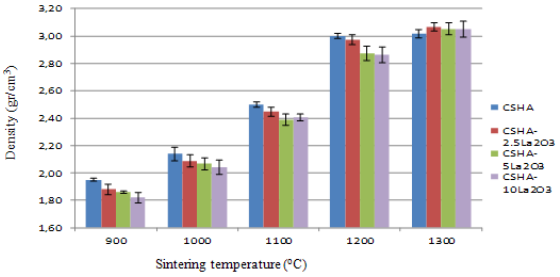

Fig. 3. The effect of sintering temperatures on the density values of the sintered samples.

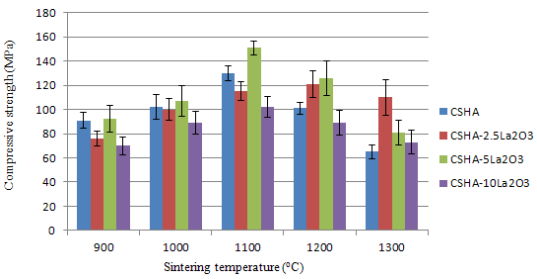

Fig. 4. Compressive strength of the sintered samples as a function of sintering temperature.

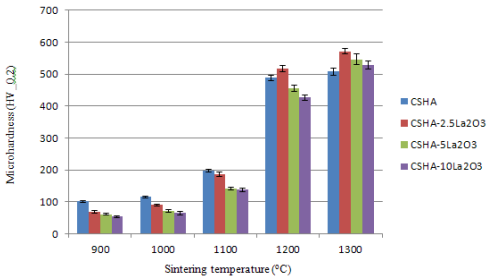

Fig. 5. Microhardness values of the sintered samples as a function of sintering temperature.

generally higher strengths compared to pure CSHA which may explain by the decreasing of second or third undesirable phase's rates via La_2O_3 reinforcement and due to its reducing effect on the grain growth of HA. Hardness of the sintered ceramics are affected by average grain size, porosity rates and second and/or third phases. As shown in Fig. 5, the hardness values of the samples increase by ascending sintering temperatures. For all sintering temperatures, the highest microhardness values were measured for CSHA-2.5La_2O_3 samples which may explain by lower porosity values, higher grain sizes and lower glassy phases.

4. Conclusion

The following conclusions can be drawn from the present study:

The mechanical properties of CSHA can be improved by the reinforcement of La_2O_3.

The optimum La_2O_3 rate was found 5% for CSHA-La_2O_3 composites to obtain higher compressive strength.

The best compressive strengths for all samples were obtained at 1100 °C, however, at higher temperatures compressive strengths of the samples decreased due to occured undesirable second and/or third phases such as CaO, TCP and whitlockite.

Acknowledgments

This work was supported by the Scientific Research Project Program of Marmara University Project No: FEN-C-YLP-130313-0087.

References

[1] F.N. Oktar, *Ceramic. Int.* **33**, 1309 (2007).

[2] C.Y. Ooi, M. Hamdi, S. Ramesh, *Ceramics International* **33**, 1171 (2007).

[3] N. Demirkol, O. Meydanoglu, H. Gokce, F.N. Oktar, E.S. Kayali, *Key Eng. Mat.* **493**, 588 (2012).

[4] A.J. Ruys, M. Wei, C.C. Sorrell, M.R. Dickson, A. Brandwood, B.K. Milthome, *Biomaterials* **16**, 409 (1995).

[5] M.K. Herliansyah, M. Hamdi, A.I. Ektessabi, M.W. Wildan, J.A. Toque, *Mat. Sci. Eng. C* **29**, 1674 (2009).

[6] G. Göller, F.N. Oktar, *Mat. Lett.* **56**, 142 (2002).

[7] C. Kailasanathana, N. Selvakumar, *Ceramic. Int.* **38**, 3569 (2012).

[8] Huaxia Ji, P.M. Marquis, *Biomaterials* **13**, 744 (1992).

[9] C.Y. Tana, A. Yaghoubia, S. Ramesha, S. Adzilaa, J. Purbolaksonoa, M.A. Hassana, M.G. Kutty, *Ceramics Int.* **39**, 8979 (2013).

[10] F.N. Oktar, S. Agathopoulos, G. Goller, H. Gökçe, E.S. Kayali, S. Salman, *Key Eng. Mat.* **330**, 411 (2007).

[11] Y. Zhang, L. Chen, J. Zeng, K. Zhoa, D. Zhang, *Mat. Sci. Eng. C* **39**, 143 (2014).

[12] British Standard Non-metallic Materials for Surgical Implants. Part 2. Specification for ceramic materials based on alumina, BS 7253: Part 2: 1990.

[13] F.N. Oktar, S. Ozyegin, O. Meydanoglu, H. Aydin, S. Agathopoulos, G. Rocha, B. Sennaroglu, S. Kayali, *Key Eng. Mat.* **309**, 101 (2006).